Design, analysis and optimization of anisogrid composite lattice conical shells

Valerio G. Belardi[a], Pierluigi Fanelli[b], Francesco Vivio[a,*]

[a]Department of Enterprise Engineering - University of Rome Tor Vergata, Via del Politecnico, 1, 00133, Rome, Italy
[b]DEIM, University of Tuscia, Largo dell'Università, 01100 Viterbo, Italy

Abstract

A methodology for structural analysis and optimal design of conical anisogrid composite lattice shell structures subject to different external loads concurrently applied and multiple stiffness constraints is presented. The critical buckling load of the anisogrid lattice conical structure is exactly assessed, independently of the buckling failure mode, by means of a discrete approach. The method makes use of a full FE parametric modeling technique able to manage all the geometrical parameters of the anisogrid composite lattice structure. Additionally, the genetic algorithm NSGA-II is employed to set up an optimization procedure which allows to analyze different sets of geometrical variables, both continuous and discrete, to reach the optimal solution in terms of mass amount and fulfilling of structural and stiffness requirements, aiming at the preliminary design of an actual structure. Numerical case-studies are outlined in order to demonstrate the practical usefulness and versatility of the proposed procedure to industrial cases where the anisogrid lattice conical structure undergoes multiple external loads and various stiffness constraints must be satisfied.

Keywords: A. Carbon Fiber, B. Buckling, C. Finite element analysis (FEA), E. Filament winding, Genetic Algorithm Optimization

1. Introduction

Anisogrid composite lattice structures are composite grid-structures which represent an effective technical solution in the aeronautic and aerospace fields for applications that require structural components characterized by high load-bearing and stiffness capabilities as well as a low mass amount.

This kind of structures are utilized in all the principal space programs, such as the Russian one, in the framework of which the early studies were carried out [1–3]. Further research programs took place in the USA, regarding both the structural behavior [4] and the manufacturing process [5] of composite grid-structures. The interest of the Japan Space Agency about this topic is likewise growing, aiming to the production of a future launchers generation [6, 7].

Launcher components such as rocket interstages, payload adapters and fairings have been realized making use of anisogrid structures and the possibility of employing them in the production of fuselage barrels is further being studied [8].

Anisogrid lattice structures consist of a repetitive arrangement of unidirectional helical and hoop composite ribs, mutually intersecting, wherein an elementary lattice cell can be identified and considered as the fundamental unit of the anisogrid structure. Anisogrid lattice structures can be found in the form of cylindrical or conical lattice shells, depending on the particular application. Hexagonal and triangular elementary lattice cells are commonly employed: in the first one, the hoop ribs divide equally the helical ribs segments spanning between adjacent intersection points; in the latter, the hoop ribs crosses the helical ribs in proximity of their intersection points. Furthermore, in [9] the skin-added X-lattice composite structure is presented: this new design solution avoids the use of hoop ribs introducing an external thin skin, with fibers in the hoop direction, to increase the mechanical performance. The external skin contributes to prevent buckling modes characterized by local rotations of the helical ribs.

One of the main issues linked to this technology is the connection of its composite endings to metallic flanges through demountable joints; this issue is currently studied by the same authors [10–13].

According to the design process, the goal is the identification of the optimal anisogrid composite lattice structure configuration, i.e. the layout with the lowest mass amount capable of fulfilling the set of constraint conditions which in general concern with static strength, buckling resistance and stiffness requirements. Different optimization methodologies can be found in literature, which concern with cylindrical and conical lattice shells and both typologies of cells. These methodologies can be divided in continuous approaches and discrete approaches.

The continuous approaches to the structural analysis of anisogrid lattice structures are based on smearing techniques, i.e. the lattice shell is treated as a continuum media: the stiffness properties of an equivalent orthotropic shell are obtained from the anisogrid lattice structure ones according to a particular criterion. These methods have been used for different purposes, such as the preliminary design of axisymmetric lattice shells reaching analytical closed form solutions regarding the optimal geometrical configuration of both cylindrical and lattice conical shells under axial compressive load [1, 14]. A numerical optimization procedure was used for anisogrid lattice

*Corresponding author. Tel.: +39 06 72597123.
Email address: vivio@uniroma2.it (Francesco Vivio)

cylindrical shells in [15] to add the axial stiffness requirement to the set of analytically formulated structural constraints applied in [1]. A similar numerical approach, but without constraints related to the stiffness of the lattice shell, was developed in [16]. Furthermore, the continuous approach was used for buckling analysis of cylindrical lattice structures [17], buckling analysis of anisogrid plates with clamped edges with various loading conditions [18, 19] and for the optimization of longitudinally compressed anisogrid lattice panels [20]. Moreover, the deformability of the anisogrid lattice structure can be analyzed exploiting the orthotropic shell theory supplied with the equivalent stiffness properties: in [21] an analytical formula to assess the axial displacement of anisogrid lattice cylindrical shells undergoing axial compression was obtained and in [22] the analytical expressions for flexural, torsional and axial global stiffness properties for anisogrid lattice conical shells are expressed.

The critical load for local and global buckling for advanced grid-stiffened carbon-fiber conical shells undergoing uniform external transverse pressure is analytically derived by means of the minimum potential energy principle in [23]. The method exploits an equivalent stiffness model which takes into account the non-uniform grid disposition. In addition, a hybrid genetic algorithm is utilized to perform the optimal design of the advanced grid-stiffened conical shell.

Sofiyev in [24] discusses a closed-form solution for buckling of heterogeneous orthotropic conical shells under external pressures; the theoretical model is formulated in the frame of the first-order shear deformation shell theory and the partial differential equations are solved through the Galerkin method. The effect on the critical pressure of the semi-vertex angle, radius-to-thickness ratio, orthotropy ratio and heterogeneity factor are parametrically explored.

The effect of temperature on buckling resistance of functionally graded material conical shells is investigated in [25]. The method is developed taking into account the Donnel shell theory, moreover non-linear temperature rise across the thickness is considered. the effect of transverse shear deformations and of geometric parameters on the buckling occurrence are investigated.

Anyway, continuous approaches can be applied for the preliminary design of axially compressed anisogrid structures, meanwhile they cannot address the analysis of different or mixed loading conditions. In addition, the ribs-density level of the lattice shell has a significant influence on the results accuracy, i.e. an adequately dense system of ribs is required as prerequisite to apply these techniques. Moreover, the continuous approaches present the intrinsic limit of taking into consideration the onset of a limited number of critical buckling modes which can affect the integrity of the anisogrid structure, i.e. the global one, typical of the orthotropic shells, and the local one, which interests the helical ribs segments delimited by two consecutive intersection points. As described in [26], further buckling modes can occur, causing the structure to collapse for a critical buckling load lower than the one predicted by the continuous approach.

Otherwise, the design methods concerning with the discrete approach mainly exploit the Finite Element Method. It can be applied to the design of anisogrid lattice structures leading to exhaustive analysis of the anisogrid lattice shell, both in terms of elastic behavior and estimation of critical load for the first buckling mode onset; however, this technique implies a higher computational effort. In [27, 28] parametric analyses are carried out to evaluate the influence of the design parameters on the structural performance of cylindrical and conical anisogrid lattice structures respectively.

Ansari and Torabi [29] developed a numerical method in order to analyze the buckling and vibration behavior of axially-compressed functionally graded carbon nanotube-reinforced composite conical shells using the variational differential quadrature method. The extended rule of mixture is employed to define the material properties of the functionally graded conical shells that are supposed smoothly varying along the thickness direction. The discretized matrix form of the Hamilton's principle is written for the problem in the framework of the first order shear deformation theory. Results are compared with the literature's ones; it is found that the buckling and vibration characteristics of the functionally graded conical shells are influenced by the volume fraction and the distribution of CNTs, boundary conditions and various geometrical parameters.

The optimization of fiber-reinforced laminated truncated conical shells is described in [30], the target is represented by the maximization of the critical buckling load acting on the fiber orientations. The golden section method is the technique chosen to perform this study. Different parametric analyses were conducted to assess the dependence of the buckling resistance on the boundary conditions, geometrical features and cutout size.

A numerical procedure for the optimization of anisogrid lattice structures is outlined in [31]; the methodology employs a FE software that is supplied with a CAD model of the structure and a genetic algorithm.

In [26] a full parametric FE model of anisogrid cylindrical lattice shells was developed and combined with the genetic algorithm NSGA-II in an optimization workflow. The FE parametric procedure generates the model taking as input the geometrical variables of the lattice shell, making use of beam elements, that are furnished by the genetic algorithm that manages the analyses to reach the structural optimization of the lattice shell in conformity with structural and stiffness constraints.

The present work aims to expand the methodology presented in [26] encompassing the anisogrid lattice conical shells to get a comprehensive design methodology capable of giving precise insights of the buckling behavior for every loading condition and facing all the requirements concerning the design of these structures. The proposed procedure uses a complete parametric modeling of the conical configuration of the structure that has been completely coupled with an optimization technique based on an NSGA-II genetic algorithm. In this way it is possible to overcome all the limitations of the continuous approaches concerning the assessment of the buckling failure and those of the discrete approaches which accurately describe the structural behavior of the anisogrid lattice structure but that have been exploited with still limited optimization margins. Using the discrete approach to accurately evaluate the critical buckling load in the design analysis, irrespective of the particular failure mode, it is possible to perform a complete and exhaustive description of the buckling failure of anisogrid lattice structures, considering all possible buckling modes, connected to different load conditions, including those that cannot be properly described through an analytical formulation and thus reliably optimize the lattice shell.

A structural optimization procedure which takes into account the simultaneous application of different load typologies and introducing multiple stiffness constraints has been defined; the consolidated condition on axial stiffness can be added to bending and torsional stiffnesses.

The proposed procedure has been apply to some numerical examples related to actual industrial cases, considering multiple external loads and stiffness constraints applied simultaneously to the anisogrid lattice conical structure.

2. Parametric modeling technique

An efficient and adaptable FE parametric modeling technique for anisogrid lattice conical structures was developed in order to feed the structural response of the lattice shell to the genetic algorithm NSGA-II, setting up an optimization workflow based on the interaction between the FE software and the NSGA-II. The FE parametric model is realized with two-noded beam element having six degrees of freedom per node.

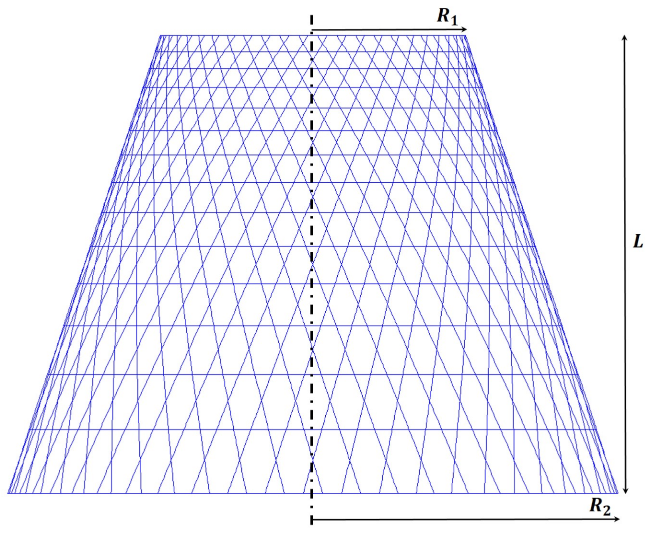

Figure 1: Anisogrid lattice conical structure composed of hexagonal elementary lattice cells.

For a generic design problem involving anisogrid lattice conical shells (Fig. 1), the global geometrical dimensions of the conical structure are defined, i.e. the smaller and the larger radii, R_1 and R_2 respectively, and the height L in conjunction with the material properties of the ribs. On the contrary, the design objective is the definition of the helical and hoop ribs arrangement, i.e. the number of ribs, as well as their cross-section dimensions.

For this purpose, five geometrical variables are used in the parametric characterization of the lattice conical shell to completely define the FE model geometry. In particular, two of them are discrete variables represented by positive and integer numbers:

- n_h the number of helical ribs with the same sense of winding;
- n_c the number of hoop ribs.

In addition, three continuous variables are needed to define the rectangular cross-section's dimensions of the two typologies of ribs (Fig. 2a):

- h the radial thickness;
- δ_h the helical ribs width;
- δ_c the hoop ribs width.

During the manufacturing process, the helical ribs are realized placing the carbon fibers along geodetic trajectories on the conical surface of the lattice shell. To define the FE parametric procedure, an analytical identification of the geodetic curve on the conical surface representing the helical ribs mid-line is implemented. The generic equation of the geodetic curve that must be characterized according to the specific set of geometrical variables. For the anisogrid conical structures the angle between the helical ribs and the meridian curve of the conical surface changes continuously along the helical rib mid-line. As a consequence the elementary lattice cell does not preserve its dimensions and geometrical proportions across the structure. This makes more complex its analytical description with respect to the cylindrical case. The analytical expression describing the helical rib mid-line (Fig. 3a) in the cylindrical coordinate system with origin at the larger end of the lattice conical shell, on the axis of symmetry, can be derived considering three geometrical relationships [14]:

$$\frac{rd\vartheta}{dl} = \tan\phi(r) \tag{1}$$

$$\frac{dr}{dl} = \sin\alpha \tag{2}$$

$$r\sin\phi(r) = C_0 \tag{3}$$

where, as also reported in Fig. 2c, r represents the generic cone radius evaluated in a plane orthogonal to the axis of the structure, ϑ is the latitude angle evaluated with respect to a reference meridian plane, $\phi(r)$ is the angle between the helical ribs mid-line and the meridian curve of the conical surface at a generic radius r, α is the cone's semi-opening angle and l is a coordinate along the meridian curve. Note that Eq. (3) is the Clairaut Equation which is valid for a geodetic curve lying on a surface of revolution.

Taking into account Eqs. (1-3), a differential equation that relates the latitude angle ϑ and the generic radius r can be determined. This relation must be integrated to get the final expression of the helical rib mid-line:

$$\int_{\vartheta_0}^{\vartheta} d\vartheta = -\int_{R_2}^{r} \frac{C_0}{r^2\sqrt{1-\frac{C_0}{r^2}}}\frac{dr}{\sin\alpha} \tag{4}$$

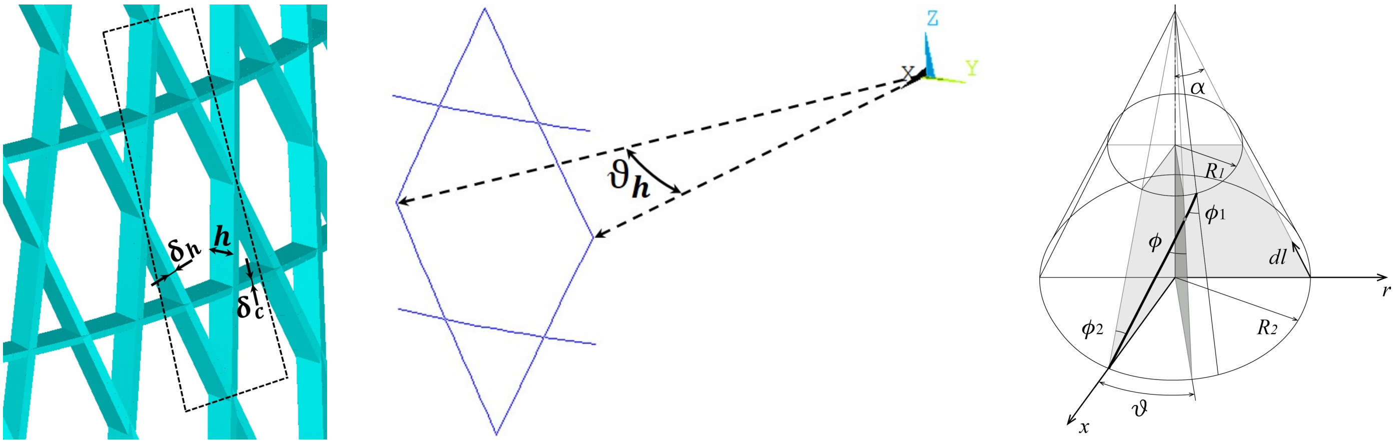

(a) (b) (c)

Figure 2: (a) Geometry of hexagonal elementary lattice cell. (b) Angle ϑ_h between two consecutive helical ribs intersection points. (c) Geometrical variables of the lattice conical shell.

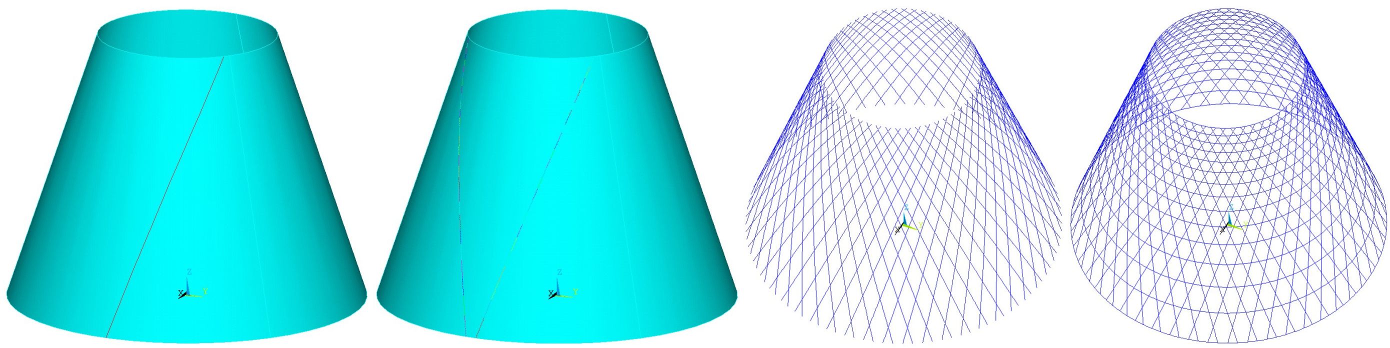

(a) (b) (c) (d)

Figure 3: (a) Geodetic curve on conical surface defining the helical ribs mid-line; (b) the two geodetic curves, one for every sense of winding, after cutting; (c) mesh of helical ribs; (d) complete mesh of anisogrid lattice conical structure.

In Eq. (4) ϑ_0 is the initial shift that is responsible of the anisogrid conical structure layout; in fact, the configuration with extremal hoop ribs is characterized by $\vartheta_0 = \vartheta_h/4$, where ϑ_h is the angle between two consecutive helical ribs intersection points (Fig. 2b), meanwhile the arrangement delimited by the overlapping areas between helical ribs has a null initial shift ϑ_0; R_2 is the larger radius of the lattice conical shell.

The final expression of the geodetic curve on conical surface, obtained integrating Eq. (4), and expressing the conical radius r as a function of the angle ϑ is:

$$r(\vartheta) = C_0 \sqrt{\frac{2}{1 + \sin\left(2 \sin\alpha(\vartheta - \vartheta_0) + \arcsin\left(\frac{2C_0^2 - R_2^2}{R_2^2}\right)\right)}} \quad (5)$$

The constant C_0 in Eq. (5) must be computed according to the overall geometry and the specific couple of discrete variables. In particular, it can be evaluated through Eq. (3) at the smaller or larger radius of the lattice conical shell where both the radius r and the inclination angle ϕ are known. The expressions for the angles between the helical rib and the meridian curve ϕ_1 and ϕ_2, at the smaller and at the larger diameter were derived by Vasiliev et al. in [16]:

$$\phi_1 = \tan^{-1}\left(\frac{R_2 \sin\gamma}{R_2 \cos\gamma - R_1}\right) \quad (6)$$

$$\phi_2 = \phi_1 - \gamma \quad (7)$$

where $\gamma = \pi \sin\alpha \frac{n_c - 1}{n_h}$.

Once Eq. (5) has been particularized for the specific anisogrid conical structure under design, the FE parametric procedure draws two helical rib mid-line, one for every sense of winding on the conical surface, realizing a set of geometrical points which are then interpolated by means of spline curves. The next operation requires the execution of a series of cuts, performed with geometrical planes orthogonal to the lattice structure axis, needed to manage the mesh generation; this operation provides nodes in correspondence of the intersection points between two helical ribs and between a helical rib and a hoop rib (Fig. 3b).

Afterwards, the proper cross-section features are assigned to the lines obtained cutting the two helical ribs mid-line and copied n_h times around the lattice shell axis (Fig. 3c). Additionally, the characteristic twist of the helical ribs cross-section alongside its mid-line is achieved acting on the the beam elements third node that regulates its coordinate system orientation with respect to the the global one.

To complete the FE model, n_c circumferences are drawn in correspondence to the hoop ribs position, each one composed of circular segments that can be enclosed between two geometrical points of intersection with helical ribs determined with the cut series. Following, the FE procedure meshes the hoop ribs curves completing the anisogrid lattice conical structure mesh as reported in Fig. 3d. When the model generation phase is complete the overall mass M can be easily evaluated.

3. Optimization workflow based on NSGA-II genetic algorithm

The proposed design methodology consists in an automatic workflow capable of determining the optimal structural configuration, ensuring the validity of a fixed number of requirements, of anisogrid lattice conical structures exploiting an FE software equipped with the aforementioned FE parametric procedure. FE analyses are executed in conjunction with the NSGA-II genetic algorithm [32], also available in many optimization commercial software packages. In particular, NSGA-II is an elitist nondominated sorting-based genetic algorithm and no training is necessary for its application. This algorithm is suitable to manage with constrained single or multi-objective optimization problems involving discrete and continuous variables. Hereafter, it is employed for single-objective analyses requiring mass minimization and the verification of structural and stiffness constraints.

Any sample analyzed by the FE software must fulfill four constraints whose validity is checked by the NSGA-II to be accepted as a possible solution; the constraints are expressed as the following inequalities:

- (I) Material compressive strength
$$\sigma_{MIN} \leq \sigma_0^C;$$
- (II) Material tensile strength
$$\sigma_{MAX} \leq \sigma_0^T;$$
- (III) Buckling resistance
$$\lambda_1 \geq 1;$$
- (IV) Minimum level of stiffnesses
$$S_i \geq S_i^{MIN}.$$

According to the constraints (I) and (II), they deal with the static strength of the anisogrid lattice conical structure, i.e. the action of external loads must not provoke the ribs' material failure. Specifically, these conditions state that the highest compressive and tensile stresses, σ_{MIN} and σ_{MAX} respectively, must not exceed the material's compressive and traction strengths (σ_0^C and σ_0^T). The stress evaluation is performed not taking into account local effects connected to constraint and load conditions. On the contrary, the analytical approaches neglect the material failure caused by the tensile stress state and exclusively admit the compressive stress as responsible of the static failure [1, 15].

Additionally, in general, the anisogrid structures mainly undergo compression loads that are responsible of a compression stress state in the helical ribs, meanwhile the hoop ribs are subjected to a traction stress state. The traction stress state acting in the hoop ribs considerably prevents the occurrence of the buckling failure since it contributes to preserve the original circular cross-section of the structure, being reason of the substantial buckling strength featured by the anisogrid structures.

In order to assure the structural strength, the resistance to the buckling onset is further considered by means of the constraint (III). In particular, the requirement is formulated stating that the first eigenvalue λ_1 obtained by finite element eigenvalue buckling analysis must be greater or equal to one. Consequently, exploiting the discrete approach, the formulation of this constraint is achieved regardless a specific buckling failure mode, i.e. it is as generic as possible, since it embraces all buckling modes that the anisogrid lattice structure can experience.

This specific expression of the buckling resistance constraint overcomes the limits of the buckling strength prediction capability proper of the analytical approaches, which account for a limit set of possible critical buckling modes as responsible of the structure's failure. This hypothesis affects the prediction of the critical buckling load and consequently the integrity of the overall structure, as outlined in [26]. In fact, on the one hand the analytical approaches analyze the anisogrid lattice structure as a continuum media through the introduction of equivalent smeared stiffness properties, i.e. it is supposed to behave as an orthotropic shell which undergoes global buckling failure. Likewise, the overall structure is considered as a three-dimensional frame which can fail because of local instability. However, the anisogrid lattice structure frequently undergoes buckling modes other than those expected by the analytical approaches; these modes are associated with its dual features that are a combination of the shell and beam-framework's ones. As a consequence, this simplified estimation of the buckling failure may result in overestimated assessment of the critical buckling load and subsequently provide a design of the structure that miss the conformity with the buckling resistance requirement.

Furthermore, the optimization work-flow can also manage functional constraints, which do not concern the structural integrity, such as those related to stiffness requirements. Indeed, anisogrid lattice structure must commonly feature controlled levels of stiffness, especially when it is a crucial part of a particular application.

The optimal solution identified by the NSGA-II is determined within the design space that is defined through the imposition of minimum and maximum values of the five variables needed to completely define a configuration of the anisogrid lattice structure.

Moreover, the genetic algorithm is supplied with a design of experiments (DOE): the algorithm analyzes an initial popu-

Table 1: The four load cases and their loading conditions and stiffness constraints.

Load Case 1 (LC1)	**Load Case 2 (LC2)**	**Load Case 3 (LC3)**	**Load Case 4 (LC4)**
Loading Conditions			
Axial Compression	Axial Compression Transverse Bending Force	Axial Compression Bending Moment	Axial Compression Torque Moment
Stiffness Constraints			
Axial Stiffness	Axial Stiffness Transverse Bending Stiffness	Axial Stiffness Bending Stiffness	Axial Stiffness Torsional Stiffness

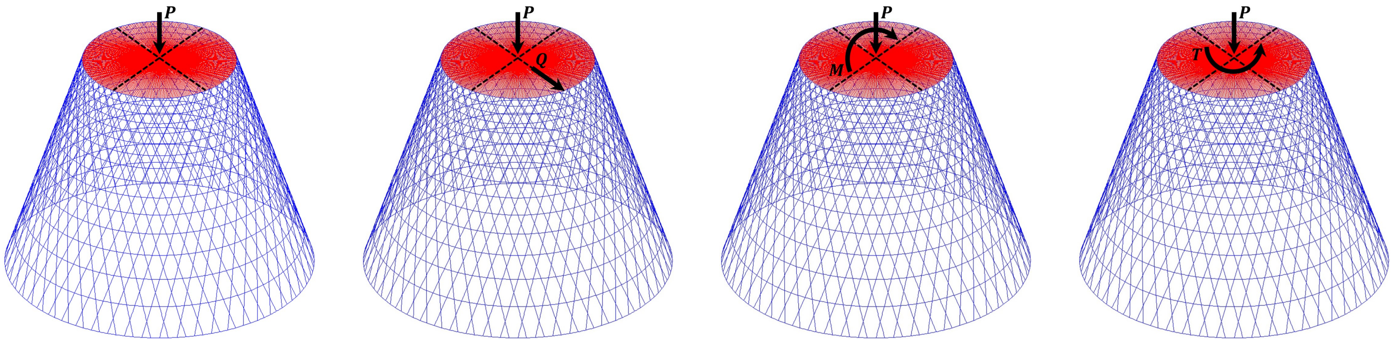

(a) (b) (c) (d)

Figure 4: Loads acting on the anisogrid conical lattice structure in: (a) Load Case 1; (b) Load Case 2; (c) Load Case 3; (d) Load Case 4.

lation of samples, selected in the design space, to estimate the structural behavior of the anisogrid lattice structure and start the automatic process of samples' generation aimed at the search of the optimum. The initial population of samples is determined by means of the Uniform Latin-Hypercube DOE technique [33] that furnishes a uniform and random distribution of samples in the design space.

Fig. 5 outlines the logical workflow employed for the optimization process of anisogrid lattice structures, that is iteratively repeated during the overall analysis. At the beginning of every computing loop, the genetic algorithm NSGA-II defines a set of geometrical variables that is transmitted to the finite element code by means of an input file. Then, the FE software executes the analysis: the pre-processor generates the FE model according to the procedure described in Section 2 and evaluates the mass M of the structure. Then, the bottom hoop rib of the FE model is clamped and a set of rigid links (shown in Fig. 4), connecting the nodes belonging to the upper extremal hoop rib to the one present in its geometrical center, where external loads are applied, is realized.

The successive step consists in the finite element eigenvalue buckling analysis and the output variables, i.e. anisogrid lattice structure's mass M, highest compressive stress σ_{MIN}, highest tensile stress σ_{MAX}, first eigenvalue λ_1 and stiffness values S_i, are reported in an output file. Afterwards, the computing loop is closed providing the output file to the genetic algorithm. The NSGA-II verifies the fulfillment of the constraints and identifies the set of input variables for the next iteration; the optimization process ends when the predefined number of samples to be analyzed has been reached. The configuration of anisogrid lattice structure featuring the lowest mass amount and satisfying all the required constraints is the optimal solution.

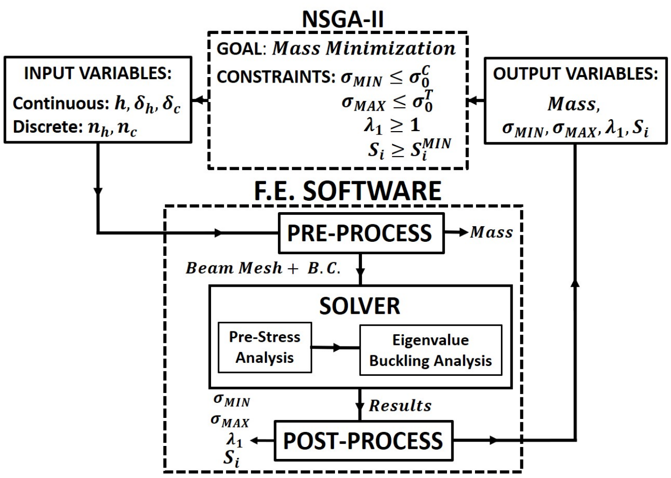

Figure 5: Logical workflow of the optimization procedure based on the finite element method coupled with the genetic algorithm NSGA-II.

4. Results

The results hereafter presented regard optimization analyses of an anisogrid lattice conical structure featuring hexagonal elementary lattice cells and delimited by extremal hoop ribs. The geometrical characteristics are: small radius $R_1 = 0.5$ m, large radius $R_2 = 1$ m and height $L = 1.5$ m. The unidirectional composite ribs are made of epoxy matrix and carbon fiber directed as the ribs, the composite material properties are: Young modulus $E = 100$ GPa, compressive strength $\sigma_0^C = 450$ MPa, tensile strength $\sigma_0^T = 600$ MPa and mass density $\rho = 1,500$ Kg/m^3. Furthermore, being the material properties highly dependent on the manufacturing process, the ribs were modeled with isotropic material for simulation purposes. The ribs Young Modulus is that evaluated along the ribs trajectories, which can be determined by means of experimental tests on specimens extracted from the overall structure.

The present Section reports some case-studies in order to exhibit the efficiency and the accuracy of the optimal design methodology here presented. The numerical examples involve the optimal design of anisogrid lattice conical structures in operating conditions, i.e. experiencing, simultaneously, different load typologies and stiffness constraints. The four load cases analyzed are graphically represented in Fig. 4. The first one concerns the action of an axial compression load and, in addition, a requirement on the axial stiffness must be satisfied. Next, the subsequent case-studies are defined superimposing one load condition and stiffness constraint at a time to the first load case.

The analyses are performed in a broad design space to prove the effectiveness and the capabilities of the genetic algorithm NSGA-II. The design space is obtained fixing the minimum and maximum values of the geometrical variables that are listed in Table 2.

Table 2: Range variation of problem's variables defining the design space.

	h [mm]	δ_h [mm]	δ_c [mm]	n_h [−]	n_c [−]
MIN	7.00	2.30	2.30	15	5
MAX	25.00	17.00	17.00	65	30

4.1. Compression axial load and axial stiffness constraint (LC1)

This load case requires the design of an anisogrid lattice conical structure, with the dimensions and the material properties previously assigned, to sustain the axial compressive load $P = 3.5$ MN. Additionally, the design must present a minimum axial stiffness $S_A = 550$ MN/m, intended as the ratio between the external load P and the maximum axial displacement in the z direction u_z^{MAX} experienced by the upper hoop rib of the lattice shell. The loading values represent typical design target in aerospace applications.

The application of the optimization methodology, which exploits the FE parametric modeling technique and the genetic algorithm NSGA-II, determined a minimum mass design satisfying the structural and the stiffness constraints. The optimal design characteristics in terms of geometric variables and structural performance are reported in Table 3.

The most heavy requirements for the sizing resulted to be the buckling and the stiffness ones: the first eigenvalue reached the unity and the axial stiffness of the lattice shell is slightly higher than the required value, whereas the failure modes related to the ribs static strength were not critical for the design; indeed the safety factor for the compressive strength is 1.20 and the one for the tensile strength is 2.93.

The anisogrid lattice shell fails because of a buckling failure mode which presents 8 lobes alternatively oriented inward and outward with respect to the lattice shell curvature (Fig. 6). The lobes are located in the lower portion of the lattice shell, above the larger extremal hoop rib. Moreover, a second series of circularly disposed lobes, featuring a less pronounced amplitude, is present over the principal one.

4.2. Transverse bending force and transverse bending stiffness constraint (LC2)

The present case-study is set up adding a transverse bending force $Q = 0.5$ MN to the compression load condition earlier analyzed; the transverse bending force acts along the x axis of the model and is applied to the upper extremal end of the lattice shell. Additionally, a transverse bending stiffness constraint must be satisfied as well as the axial one, a minimum value of $S_{TB} = 100$ MN/m is requested. This last stiffness value is computed through the ratio of the transverse bending force Q and the maximum displacement alongside its direction of application, i.e. u_x^{MAX}.

The optimization analysis performed by means of the NSGA-II allowed to find out the design parameters reported in Table 3. The action of the two external loads, along with the second stiffness requirement, asked for a mass increase of 16.01%.

According to ribs cross-section's dimensions, the thickness h and helical ribs' width δ_h are greater than those of the preceding sizing, meanwhile hoop ribs' width δ_c is decreased. Moreover, the number of helical ribs n_h is reduced and the number of hoop ribs n_c is almost unchanged.

Three constraints turned out to be a driver for the sizing of the anisogrid structure: once again the buckling failure one, since λ_1 is very close to the unity, the maximum compressive stress σ_{MIN} nearly reached its threshold value and, similarly, the transverse bending stiffness S_{TB} is very close to the minimum required value. Contrariwise, the other conditions were not stringent: the safety factor for the tensile strength is 1.41 (it is higher than the previous load case) and the axial stiffness S_A is 23.03 % higher than the minimum value.

The buckling failure mode of the anisogrid lattice structure is shown in Fig. 7; the collapse of the lattice shell takes place in the central zone of the structure, where the compression stress state provoked by the axial force is superimposed to the one due to the transverse bending force Q. In particular, the instability causes the rotation of both helical and hoop ribs in the tangential plane and it not induces any radial displacement. Anyway, the buckling occurrence is circumscribed to a region close to the larger diameter, as for the previous load case.

Table 3: Geometric parameters and finite element analysis results of the anisogrid lattice conical structure designed for the four load cases considered.

	U.o.M.	Load Case 1	Load Case 2	Load Case 3	Load Case 4
M	[Kg]	42.54	49.35	58.75	58.34
h	[mm]	18.95	20.18	18.94	22.56
δ_h	[mm]	6.22	8.71	15.92	15.12
δ_c	[mm]	4.86	3.10	3.37	3.75
n_h	[−]	55	48	36	31
n_c	[−]	16	15	10	9
σ_{MIN}	[MPa]	373.84	449.98	423.05	449.96
σ_{MAX}	[MPa]	205.03	426.17	548.00	428.31
λ_1	[−]	1.00	1.03	1.16	1.16
u_z^{MAX}	[mm]	6.12	5.17	3.81	3.93
S_A	[MN/m]	572.05	676.65	917.89	890.93
u_x^{MAX}	[mm]		4.94		
S_{TB}	[MN/m]		101.31		
rot_y^{MAX}	[rad]			$3.85 \cdot 10^{-3}$	
S_B	[MNm/rad]			130.03	
rot_z^{MAX}	[rad]				$1.39 \cdot 10^{-2}$
S_T	[MNm/rad]				72.02

4.3. Bending moment and bending stiffness constraint (LC3)

In this case-study, the bending moment $M = 0.5$ MNm is applied to the top of the lattice shell, along the y axis of the model, to enlarge the basic compression load case beforehand discussed. Likewise, a second stiffness constraint is further imposed demanding a minimum bending stiffness $S_B = 130$ MNm/rad; it is defined as ratio of the bending moment and the resulting angle of rotation rot_y^{MAX} undergone by the upper cross-section of the anisogrid lattice structure.

Table 3 presents the outcomes of the optimization performed with the proposed procedure. Compared to the first case-study involving only axial compression force and axial stiffness constraint, the presence of the double external load and stiffness constraints increases the mass by 38.11%. Furthermore, the value of the thickness h did not considerably change, helical ribs' width δ_h is greater than the one of the first sizing, while hoop ribs' width δ_c is reduced; both discrete variables are decreased.

The most strictly verified constraint condition is the bending stiffness one, indeed the optimal lattice shell features a value correlated to this property just over the minimum. The other requirements are more amply fulfilled: the compressive strength presents a safety factor of 1.06, the tensile strength a safety factor of 1.09 and the axial stiffness is abundantly greater than the imposed minimum value. The buckling failure is not critical for this sizing being the first eigenvalue λ_1=1.16.

Because of the mixed loading condition, the buckling failure occurs in the half of the anisogrid lattice conical structure where the bending moment establishes a compression stress state of the helical ribs, as shown in Fig. 8. The buckling mode is characterized by three lobes: one of them directed outward, with respect to the lattice shell curvature, and two inward.

4.4. Torque moment and torsional stiffness constraint (LC4)

The anisogrid lattice structure undergoes the action of the axial compression force and of the torque moment $T = 1$ MNm along the z axis of the model. Moreover, the stiffness constraint concerning axial stiffness was considered together with a requirement on torsional stiffness: a requested minimum value of $S_T = 70$ MNm/rad was defined. The torsional stiffness is evaluated dividing the torque moment T by the rotation rot_z^{MAX} of the upper extremal end about the axis of the lattice shell.

The results of the optimization process are reported in Table 3. The mass of the lattice shell increases of 37.14 % with respect to the baseline configuration of the first load case. Concerning to ribs cross-section's dimensions: the thickness h and helical ribs' width δ_h are greater than those of the simple compression load case, while hoop ribs' width δ_c decreased; besides, both discrete variables n_h and N are reduced.

The maximum compressive stress σ_{MIN} experienced an intensification by reason of the superposition of the axial force and the torque moment, so that it approaches the strength limit. Conversely, the tensile strength is not stringent for this design being the safety factor for this failure mode 1.40; similarly, the first eigenvalue is λ_1=1.16. Once again, the axial stiffness constraint is largely verified.

The combined action of the axial and the torsional loads makes the anisogrid lattice conical structure to buckle according to a buckling failure mode, reported in Fig. 9, characterized by 8 oblique stretched lobes alternatively oriented inward and outward with respect to the lattice shell curvature.

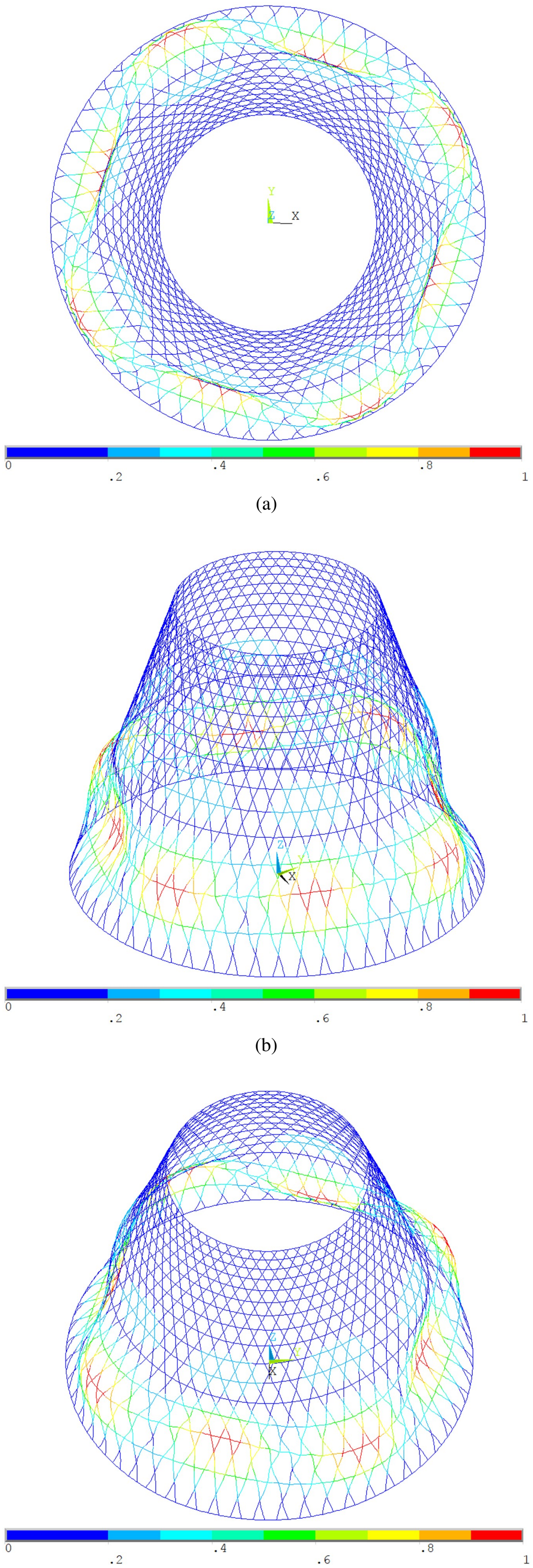

(a) (b) (c)

Figure 6: Buckling failure mode for axial compression load case (LC1), λ_1 = 1.00. Top view (a) and prospective views (b, c).

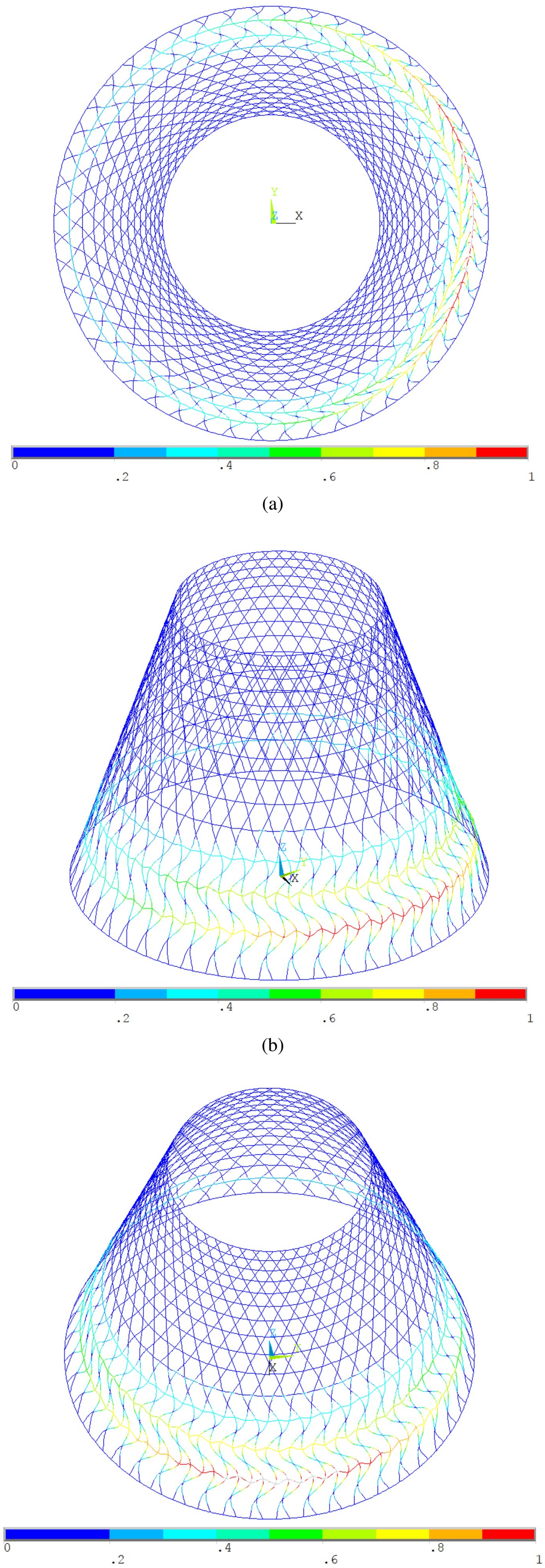

(a) (b) (c)

Figure 7: Buckling failure mode for load case (LC2) with combination of axial compression and transverse bending forces , λ_1 = 1.03. Top view (a) and prospective views (b, c).

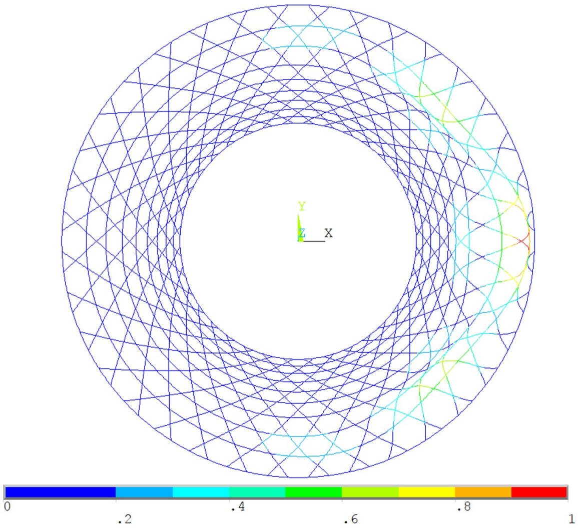

(a)

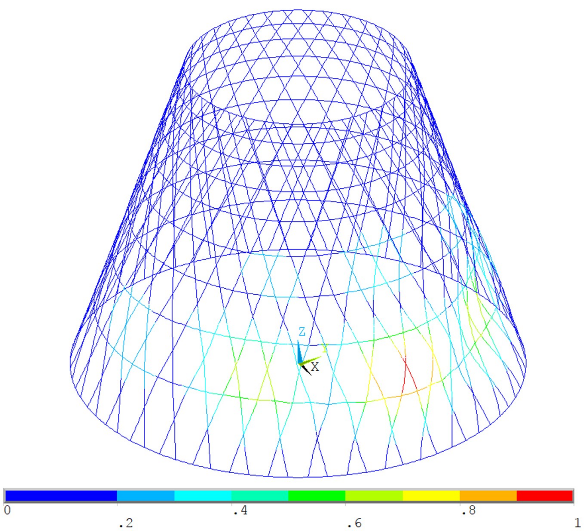

(b)

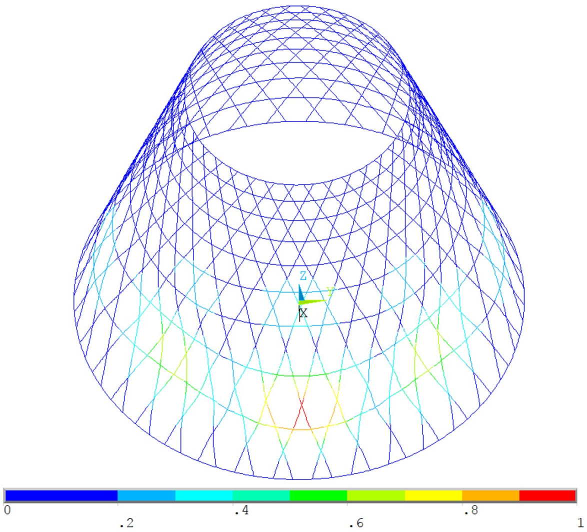

(c)

Figure 8: Buckling failure mode for load case (LC3) with combination of axial compression and bending moment, λ_1 = 1.16. Top view (a) and prospective views (b, c).

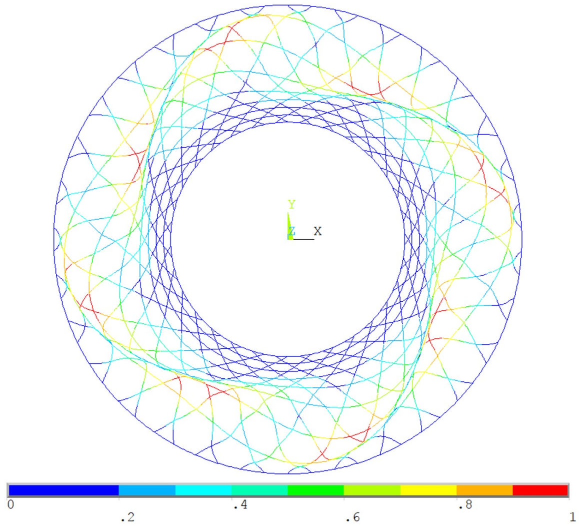

(a)

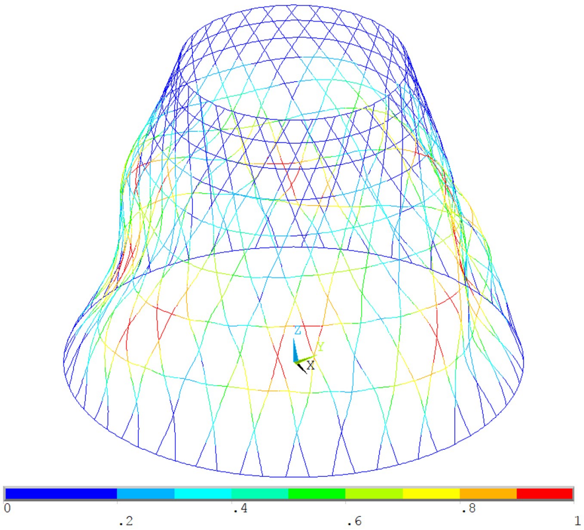

(b)

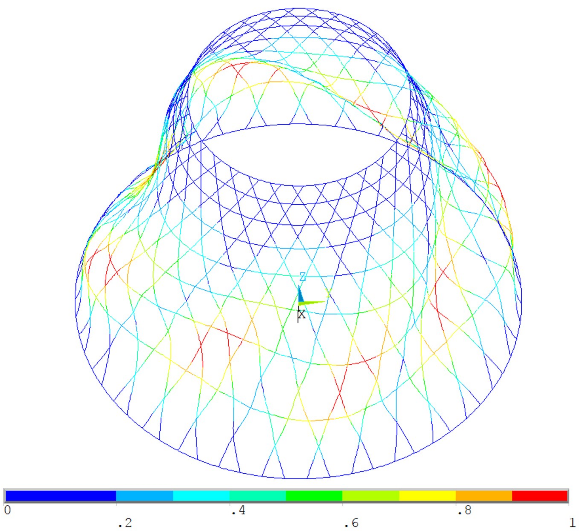

(c)

Figure 9: Buckling failure mode for load case (LC4) with combination of axial compression and torque moment, λ_1 = 1.16. Top view (a) and prospective views (b, c).

5. Conclusions

An original methodology for the design and the optimization method for anisogrid lattice conical structures was presented. The procedure allows to deduce the minimum mass configuration of the lattice conical shell undergoing multiple external loads concurrently applied and required to satisfy any kind of stiffness requirements.

The presented methodology makes use of an original parametric FE modeling technique capable of generating meshes of anisogrid lattice conical structures. Five geometrical quantities are utilized as input variables: three of them are continuous variables needed to characterize the cross-section dimensions of the unidirectional composite ribs and two represents the numbers of helical and hoop ribs. The outcomes of the FE analyses are assessed by the optimization algorithm NSGA-II that checks the compliance with the imposed requirements and determines the set of input variables for the successive analyses to be carried out.

This optimization technique enhances the buckling prediction capabilities with respect to analytical approaches for the design of anisogrid structures which take into account a restricted number of buckling failure modes. Furthermore, the possibilities of optimization are expanded to include loading conditions typical of the real operative conditions.

It is demonstrated that the proposed approach allows to overcome the typical limits of the continuous approaches concerning the incomplete description of the lattice shell buckling modes and the consequent possibility of not satisfying all the structural requirements.

The Results section reports numerical case-studies concerning applicative design problems featuring different typologies of external loads and stiffness constraints, demonstrating the accuracy of the presented method and the applicability to industrial cases.

Acknowledgments

The authors would like to acknowledge Avio Spa for the support to this work (PhD grant funding).

References

[1] V. V. Vasiliev, V. Barynin, A. F. Razin, Anisogrid lattice structures survey of development and application, Composite Structures 54 (2001) 361–70.

[2] V. V. Vasiliev, A. F. Razin, Anisogrid composite structures for spacecraft and aircraft applications, Composite Structures 76 (2006) 182–9.

[3] V. V. Vasiliev, V. Barynin, A. F. Razin, Anisogrid composite lattice structures - development and aerospace applications, Composite Structures 94 (2012) 1117–27.

[4] S. Huybrechts, S. W. Tsai, Analysis and behavior of grid structures, Composites Science and Technology 56 (1996) 1001–1015.

[5] S. M. Huybrechts, T. E. Meink, P. M. Wegner, J. M. Ganley, Manufacturing theory for advanced grid stiffened structures, Composites Part A: Applied Science and Manufacturing 33 (2002) 155–161.

[6] K. Terashima, T. Kamita, T. Aoki, T. Yokozeki, G. Kimura, T. Uzawa, Experimental study of buckling properties of composite lattice structures for launcher, in: Proc. of 16th European Conf. on Composite Materials, Sevilla, Spain.

[7] T. Aoki, T. Yokozeki, K. Terashima, T. Kamita, Mechanical Behavior of Composite Lattice Cylinders, in: 55th AIAA/ASME/ASCE/AHS/ASC Structures, Structural Dynamics, and Materials Conference.

[8] D. Liu, H. Lohse-Busch, V. Toropov, C. Hühne, U. Armani, Detailed design of a lattice composite fuselage structure by a mixed optimization method, Engineering Optimization 48 (2016) 1707–1720.

[9] T. Yokozeki, Y. Shimizu, M. Ishii, K. Kimizuka, S. Suzuki, Y. Yamasaki, K. Terashima, T. Kamita, T. Aoki, Mechanical behavior in compression of skin-added X-lattice composite panel with corrugated ribs, Composite Structures 168 (2017) 863–871.

[10] V. G. Belardi, P. Fanelli, F. Vivio, Structural analysis of transversally loaded quasi-isotropic rectilinear orthotropic composite circular plates with Galerkin method, Procedia Structural Integrity 8 (2018) 368–378.

[11] V. G. Belardi, P. Fanelli, F. Vivio, Bending analysis with Galerkin method of rectilinear orthotropic composite circular plates subject to transversal load, Composites Part B: Engineering 140 (2018) 250–259.

[12] V. G. Belardi, P. Fanelli, F. Vivio, Elastic analysis of rectilinear orthotropic composite circular plates subject to transversal and in-plane load conditions using Ritz method, In preparation (2018).

[13] V. G. Belardi, P. Fanelli, F. Vivio, Analysis of rectilinear orthotropic composite circular plates undergoing in-plane bending moment and torque through Ritz method, In preparation (2018).

[14] A. F. Rasin, V. V. Vasiliev, Development of composite anisogrid spacecraft attach fitting, in: Proc. of the 11th European Conf. on Composite Materials, Rhodos, Greece.

[15] Z. Totaro, Z. Gürdal, Optimal design of composite lattice shell structures for aerospace applications, Aerospace Science Technology 13 (2009) 157–64.

[16] V. V. Vasiliev, A. Razin, G. Totaro, F. De Nicola, Anisogrid conical adapters for commercial space application, in: AIAA/CIRA 13th International Space Planes and Hypersonics Systems and Technologies Conference.

[17] M. Buragohain, R. Velmurugan, Buckling analysis of composite hexagonal lattice cylindrical shell using smeared stiffener model, Defence Sci J 59(3) (2009) 230–8.

[18] A. V. Lopatin, E. V. Morozov, A. V. Shatov, Buckling of uniaxially compressed composite anisogrid lattice plate with clamped edges, Composite Structures 157 (2016) 187–196.

[19] A. V. Lopatin, E. V. Morozov, A. V. Shatov, Buckling of uniaxially compressed composite anisogrid lattice cylindrical panel with clamped edges, Composite Structures 160 (2017) 765–772.

[20] G. Totaro, Optimal design concepts for flat isogrid and anisogrid lattice panels longitudinally compressed, Composite Structures 129 (2015) 101–110.

[21] A. V. Lopatin, E. V. Morozov, A. V. Shatov, Axial deformability of the composite lattice cylindrical shell under compressive loading: Application to a load-carrying spacecraft tubular body, Composite Structures 146 (2016) 201–206.

[22] G. Totaro, Flexural, torsional, and axial global stiffness properties of anisogrid lattice conical shells in composite material, Composite Structures 153 (2016) 738–745.

[23] S. Shi, Z. Sun, M. Ren, H. Chen, X. Hu, Buckling resistance of grid-stiffened carbon-fiber thin-shell structures, Composites Part B: Engineering 45 (2013) 888–896.

[24] A. H. Sofiyev, Buckling of heterogeneous orthotropic composite conical shells under external pressures within the shear deformation theory, Composites Part B: Engineering 84 (2016) 175–187.

[25] A. H. Sofiyev, Z. Zerin, N. Kuruoglu, Thermoelastic buckling of fgm conical shells under non-linear temperature rise in the framework of the shear deformation theory, Composites Part B: Engineering 108 (2017) 279–290.

[26] V. G. Belardi, P. Fanelli, F. Vivio, Structural analysis and optimization of anisogrid composite lattice cylindrical shells, Composites Part B: Engineering 139 (2018) 203–215.

[27] E. V. Morozov, A. V. Lopatin, V. A. Nesterov, Finite-element modelling and buckling analysis of anisogrid composite lattice cylindrical shells, Composite Structures 93 (2011) 308–23.

[28] E. V. Morozov, A. V. Lopatin, V. A. Nesterov, Buckling analysis and design of anisogrid composite lattice conical shells, Composite Structures 93 (2011) 3150–62.

[29] R. Ansari, J. Torabi, Numerical study on the buckling and vibration of

functionally graded carbon nanotube-reinforced composite conical shells under axial loading, Composites Part B 95 (2016) 196–208.

[30] H. T. Hu, H. C. Chen, Buckling optimization of laminated truncated conical shells subjected to external hydrostatic compression, Composites Part B: Engineering 135 (2018).

[31] V. K. Maes, L. Pavlov, S. M. Simonian, An efficient semi-automated optimisation approach for (grid-stiffened) composite structures: Application to ariane 6 interstage, Composite Structures (10.1016/j.compstruct.2016.02.082).

[32] K. Deb, A. Pratap, S. Agarwal, T. Meyarivan, A fast and elitist multiobjective genetic algorithm: NSGA-II, IEEE Transactions on Evolutionary Computation 6(2) (2002) 182–197.

[33] M. D. Mckay, R. J. Beckman, W. J. Conover, Comparison of Three Methods for Selecting Values of Input Variables in the Analysis of Output from a Computer Code, Technometrics 21(2) (1979) 239–245.